Wave Propagation Fourier

Kaitlin Coleman, Simon Julien, Desmond Manthy

December 2019

Abstract

The following project is an introductory investigation on water waves and dispersive relations. There were two contrasting experiments conducted in order to show the important mechanics of water waves in different settings and circumstances. First, a physical experiment was conducted by dropping marbles into a bucket of water and observing the resulting waves. From this we were able to predict a surface tension value of around $.01\frac{N}{m}$ and create two accurate functions for phase and group velocity of the system. In the second experiment we gathered data taken from a paper where ocean waves were measured as they propagated past four different locations in the Pacific. This allowed us to discover the differences between two different dispersion relation models. It was also a thorough way to outline the accuracy and importance of using the theoretical dispersion relation to predict water wave outcomes like "time of arrival".

1 Introduction

Mathematics is an incredible tool, and perhaps most impressive, is its application in modeling the world around us. Under the assumption that water is an inviscid and incompressible fluid, water waves traveling across a bathtub, lake, or even the ocean can be modeled by dispersive waves. This application makes dispersive waves a powerful mathematical tool which we will explore throughout this project. Here we will be investigating both gravity and capillary waves, utilizing wavelength vs. depth deep-water approximations for both parts of the project. The main focus will be on the dispersive property of waves. That is, waves of different wavelengths travel at varying speeds, leading them to propagate away from a central disturbance. This follows our intuition as it can be seen in everyday life as ripples travel away from a stone cast into a pond. However, being able to understand and model the behavior of those ripples (ie. water waves) is what we hope to accomplish here.

In order to model this phenomenon, we will look to find a solution to the linearized form of the water wave equation in the x-y plane with respect to time t:

$$\eta(x,y,t) = A(k,l) * [e^{ikx-ily-i\omega(k,l)t} + e^{-ikx+ily+i\omega(k,l)t}] \tag{1}$$

In this equation $\eta(x,y,t)$ represents the height of the wave above the mean level of the water surface. The frequency of the wave is represented by $\omega(k,l)$, the amplitude of the k, l wave mode is represented by $A(k,l)$, and the variables k and l represent the wave number in the x and y directions respectively (Note the wave number is $\frac{2\pi}{\lambda}$ for respective λ in the x and y directions).

Now to understand the the difference between gravity and capillary waves we first need to understand that at the air-water boundary there are two main forces acting on the wave – gravity and surface tension. These forces affect waves differently based on the wave size. For waves with wavelengths smaller than a one or two centimetres surface tension is the dominating force (we call these capillary waves). For waves with wavelengths larger than a couple centimetres gravity is the dominating force (we call these gravity waves). The dispersion relation (the relationship between a wavelength and its frequency in a medium) for water waves is also reliant on the gravity g and surface tension σ.

Taking $\kappa = \sqrt{k^2 + l^2}$, gravity g, surface tension σ, and the water depth h, the dispersion relation is as follows:

$$\omega^2 = (g + \sigma\kappa^2)[\kappa * tanh(\kappa h)] \tag{2}$$

Another important behavior to understand it the speed at which waves travel. The peaks of water waves propagates with phase speed c_p:

$$c_p(k) = \frac{\omega(\kappa)}{\kappa} \tag{3}$$

The wave envelope propagates with groups speed $c_g(\kappa)$:

$$c_g(\kappa) = \frac{d\omega}{d\kappa} \tag{4}$$

The above equations will be derived in the following section.

1.1 Derivation

The derivation has been condensed to be more concise while still retaining all key steps. The full derivation can be found in the References [1], which this is based off.

Take the wave equation:

$$\nabla^2\Phi = \frac{1}{c^2}\frac{\partial^2\Phi}{\partial^2 t} \tag{5}$$

Note, c is the speed of sound in water $1400\frac{m}{s}$. Now shallow depths, far less than $1400m$, the wave equation can bt approximated by:

$$\nabla^2\Phi = 0 \tag{6}$$

Now let the free surface be $z = \eta(x, y, t)$. Assume a gently sloping free surface. Then, the vertical velocity of the free surface must be equal to the vertical velocity of the surface itself. This creates the relation:

$$\frac{\partial\eta}{\partial t} = \frac{\partial\Phi}{\partial z}, z = 0 \tag{7}$$

Now for any volume element, the momentum M of that element can be written as:

$$M = mu = \rho uV \tag{8}$$

Where u is the velocity of the volume element and V is the volume. The change in momentum over a distance can then be written as:

$$\frac{\partial M}{\partial x} = \rho uS \tag{9}$$

Where S is the cross sectional-area of the volume element. Then the rate of change of momentum can be written as:

$$\frac{\partial \rho u S}{\partial t} \tag{10}$$

Under the assumptions that the air above the water is stagnant with constant pressure (which is reasonable due to its very small density) and by applying the conservation of mass, and summing the pressure forces the momentum equation is obtained:

$$\rho(\frac{\partial u}{\partial t} - u\frac{\partial u}{\partial x}) = -\frac{\partial \rho}{\partial x} \tag{11}$$

Thus the linearization of the momentum equation yields:

$$\rho\frac{\partial u}{\partial t} = \frac{\partial \rho}{\partial x} = -\triangle P - \rho g e_z \tag{12}$$

Since we are operating with water which is incompressible, the total pressure can be split into static and dynamic pressures like so:

$$P = p_0 + p \tag{13}$$

Adapting the linearized momentum equation with $p_o = -\rho g z \Rightarrow \triangle p_0 = -\rho g e_z$ results in:

$$\rho\frac{\partial u}{\partial t} = -(\triangle P - \triangle p_0) = -\triangle p \tag{14}$$

Thus leading to the relationship between dynamic pressure and velocity potential:

$$p = -\rho\frac{\partial \Phi}{\partial t} \tag{15}$$

Recall that surface tension is included. Thus we adopt the model that the water has a thin film covering its surface with tension T per unit length. Now consider a horizontal rectangle $dxdy$ on the surface of the water. Then the net vertical force from four sides is:

$$(T\frac{\partial \eta}{\partial x}|_{x+dx} - T\frac{\partial \eta}{\partial x}|_x)dy + (T\frac{\partial \eta}{\partial y}|_{x+dy} - T\frac{\partial \eta}{\partial y}|_y)dx = (T\frac{\partial^2 \eta}{\partial x^2} + T\frac{\partial^2 \eta}{\partial x^2})dxdy \tag{16}$$

Continuity of the vertical forces leads to:

$$p_0 + p + T(\frac{\partial^2 \eta}{\partial x^2} + T\frac{\partial^2 \eta}{\partial x^2}) = 0 \tag{17}$$

Which leads to:

$$-\rho g\eta - \rho\frac{\partial \Phi}{\partial t} + T(\frac{\partial^2 \eta}{\partial x^2} + T\frac{\partial^2 \eta}{\partial x^2}) = 0, z = 0 \tag{18}$$

Then, from combining equations (7) and (18) get:

$$\frac{\partial^2 \Phi}{\partial t^2} + \frac{\partial \Phi}{\partial z} - \frac{T}{\rho}\nabla^2\frac{\partial \Phi}{\partial z^2} = 0, z = 0 \tag{19}$$

Take the case with a sinusoidal wave with a constant water depth and and infinitely long crests parallel to the y-axis. This creates:

$$\Phi = f(z) = e^{ikx - iwt} \tag{20}$$

Now recall that both equations (19) and (6) must be satisfied. Thus assuming inviscid flow the following differential equations must be solved:

$$f'' + k^2 f = 0, -h < z < 0 \tag{21}$$

$$-\omega^2 f + gf' + \frac{T}{\rho}k^2 = 0, z = 0 \tag{22}$$

$$f' - 0, z = -h \tag{23}$$

Solving the differential equations:

$$\Phi = Bcoshk(z+h)e^{ikx-i\omega t} \tag{24}$$

Then employing the deep water assumption, $kh >> 1$, $tanh(kh) \Rightarrow 1$, gives the dispersion relation:

$$\omega^2 = gk - \frac{T}{\rho}k^3 \tag{25}$$

Phase velocity c_p:

$$c_p = \frac{\omega}{k} \tag{26}$$

Group Velocity $c_g(\kappa)$:

$$c_g = \frac{\partial \omega}{\partial k} \tag{27}$$

Substituting k with $\kappa = \sqrt{k^2 + l^2}$, the results from the introduction are obtained.

2 ITLL Experiment

2.1 Procedure

Our first investigation into the dispersion of water waves originated with a physical experiment. In this experiment we dropped **four** marbles, of sizes 1.42cm, 1.57cm, 2.21cm, and 3.45cm, into a tub of water. By dropping these marbles into the bucket, water waves propagated outwards from the marble's point of impact at the surface of the water. With a high-speed camera, we were able to capture the wave dispersion along with a correlated time series. Using LoggerPro and video analysis software, wave displacement and wavelength were easily measured. Specifically, for every marble dropped, velocity and wavelength were measured for two separate waves and multiple points in time. After all measurements were taken, these values were averaged. This means that the resulting data of our experiment consisted of a wavelength and phase velocity value for eight individual waves (two waves were measured per marble).

2.2 Calculation of Surface Tension

Returning of data collection, wave numbers for individual waves are found from Eq. 28:

$$\kappa = \frac{2\pi}{\lambda} \tag{28}$$

Similarly, using our newfound values for κ and measured values of phase velocity ($c_p(\kappa)$), Eq. 3 gives us values for wave frequencies $\omega(\kappa)$. Water waves in a system primarily dominated by surface tension rather than gravity frequency (ω) are referred to as *capillary waves* and can be approximated as

$$\omega = \sqrt{\sigma\kappa^3} \tag{29}$$

when wavelength is shorter than the depth of the water bin (*tanh* goes to one). Comparing our frequency values from both phase speed and theoretical capillary relation calculations, we can find our desired value of surface tension $\sigma = 8.75 * 10^{-5}$. As our team continued our research we found that this is a reasonable value for σ because much work done on this subject has an accepted σ value of $7.30 * 10^{-5}$ for ideal water.

Upon further investigation based on minimum phase and group speed calculations done below, we have additionally discovered that a more realistic approximation of σ is $1 * 10^{-5}$. Lowering our surface tension value from the theoretical limit is a valid process due to the fact that the water we actually used in our experiment cannot have been ideal (probably not even close). Lowering the surface tension factor to this level allows your results to make more physical sense when plotted against our baseline minimum group and phase velocities in the following sections. Additionally, see "consistency check" section for more detailed analysis on the units of σ.

2.3 Calculation of Minimum Phase Speed

We begin our solution for the minimum wave speed c_p with the dispersion relation

$$\omega = \sqrt{g\kappa + \sigma\kappa^3}$$

Without requiring any of our measured data, the theory allows us to substitute this relation into Eq. 3 to find a function for phase speed:

$$c_p(\kappa) = \frac{\sqrt{g\kappa + \sigma\kappa^3}}{\kappa}$$

This function has a minimum as its only extrema, so solving for the roots of its derivative we found the minimum phase speed occurs at

$$\kappa = \sqrt{\frac{g}{\sigma}} = 990.4544 m^{-1}$$

At this value of κ wavelength $\lambda = 0.63cm$ and $cp_{min} = 0.1407\frac{m}{s}$ using our adjusted surface tension $\sigma = 1 * 10^{-5}$.

This is an exciting result once put into the context of the information displayed in Figures 1 & 2. For the corrected surface tension $\sigma = 1 * 10^{-5}$, we can see that our second largest marble sits on the cusp of this minimum phase speed. This is a significant find because we have found a marble size that exists at the critical turning point of wave speed propagation. For small enough objects, most of the waves generated should be capillary waves, where the shortest waves travel the fastest. For large enough objects, ie. the largest marble in our experiment, the opposite is true and the longest waves travel the fastest. By the *second to largest* marble sitting at the smallest logical phase speed, we are witnessing the turn around in dispersive behavior.

To outline the significance of our "corrected" value for surface tension we have created two plots that attempt to convey the same story. One has our original value of $\sigma = 8.75 * 10^{-5}$ and the other has the more logical results using a value of $\sigma = 1 * 10^{-5}$.

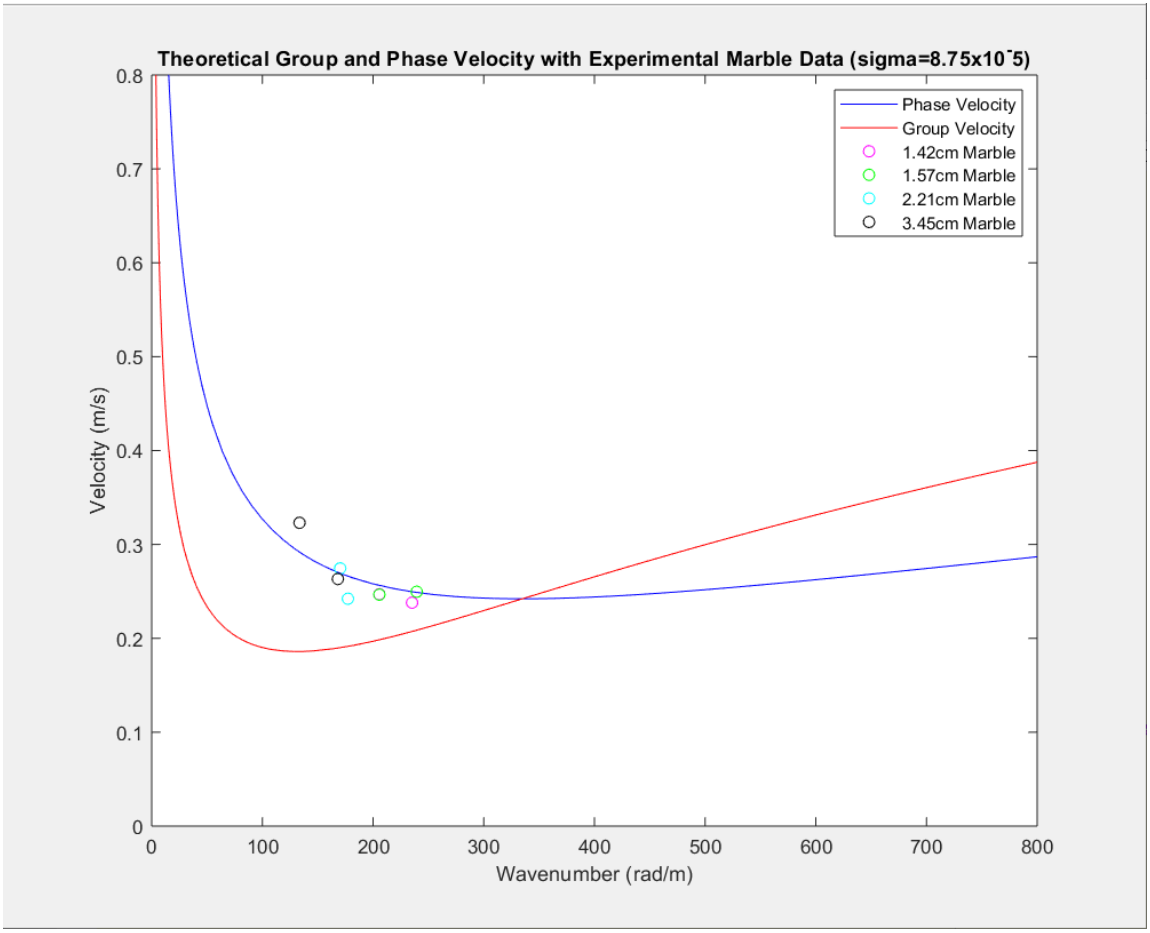

Figure 1: Phase and Group velocity functions plotted against experimentally measured wave data. With $\sigma = 8.75 * 10^{-5}$ there is an apparent issue with some waves moving slowing than the minimum phase speed.

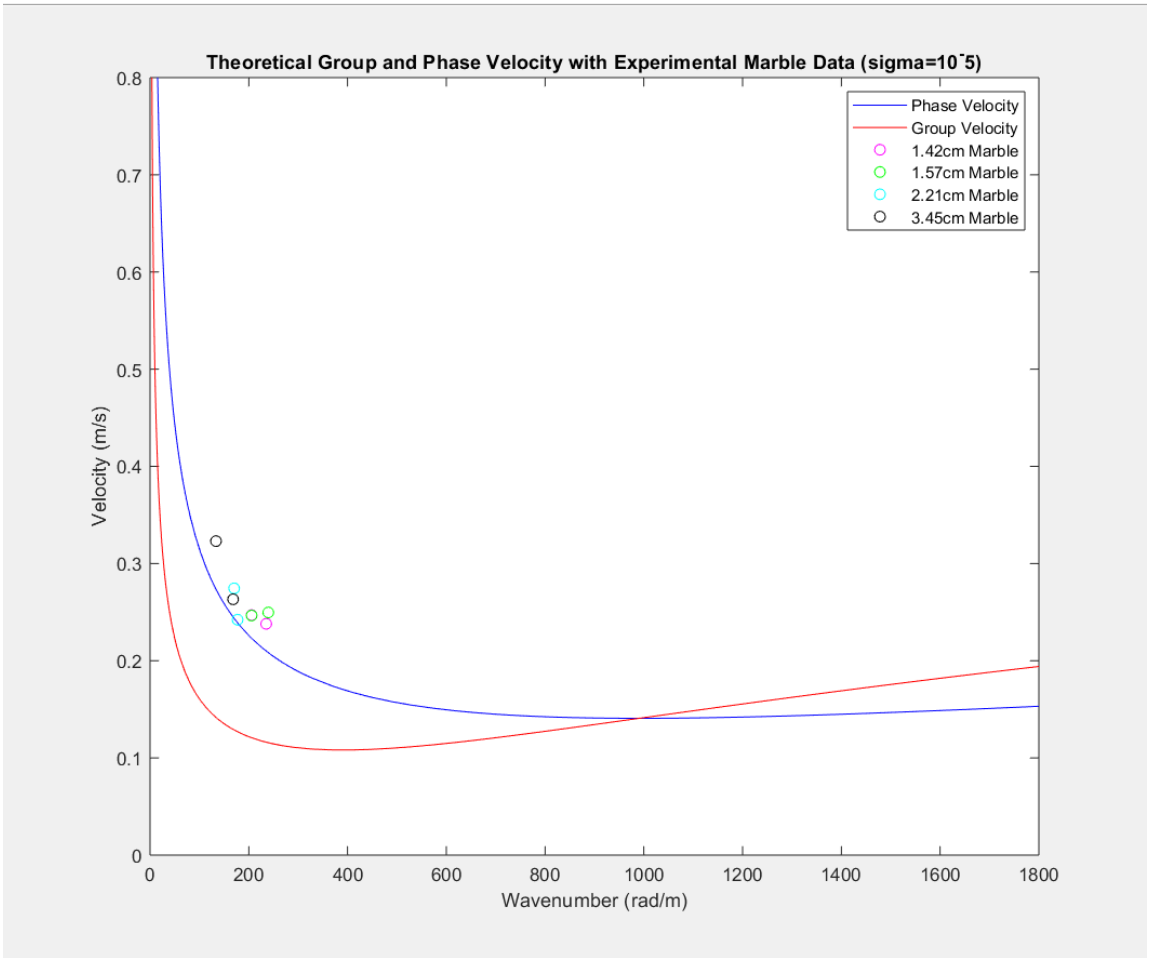

Figure 2: Phase and Group velocity functions plotted against experimentally measured wave data. With $\sigma = 1 * 10^{-5}$ the measured wave data results make much more logical sense as they all exists either above or on the minimum phase speed values. Notice specifically that the second to largest marble diameter is the one that lies essentially on top of this minimum phase speed curve.

2.4 Calculation of Minimum Group Speed

Figures 1 & 2 also show the resulting functions for the theoretical minimum group speed function. Similar to the minimum phase speed calculations, theoretical group speed also begins with the dispersion relation

$$\omega = \sqrt{g\kappa + \sigma\kappa^3}$$

Eq. 4 suggests that the group speed c_g is simply the derivative of this dispersion relation. This leaves us with the function:

$$c_g = \frac{g + 3\sigma\kappa^2}{2\sqrt{gk + \sigma\kappa^3}}$$

Again, this function only has one critical point, which is a minimum value. Thus, taking setting the derivative to 0 tells us the value of $k_{min} = \sqrt{\frac{(2\sqrt{3}-3)g}{3\sigma}} = 389.57m^{-1}$. This corresponds to a wavelength $\lambda = 1.61cm$ and group velocity $c_g = 0.1081\frac{m}{s}$ when considering $\sigma = 1 * 10^{-5}$.

Figure 3 overlays the minimum group speed function on our experimental data as a relationship of displacement and time. Logically, all of our measurements should have an average traveling velocity larger than this minimum with no information on the minimum group speed. This is true!

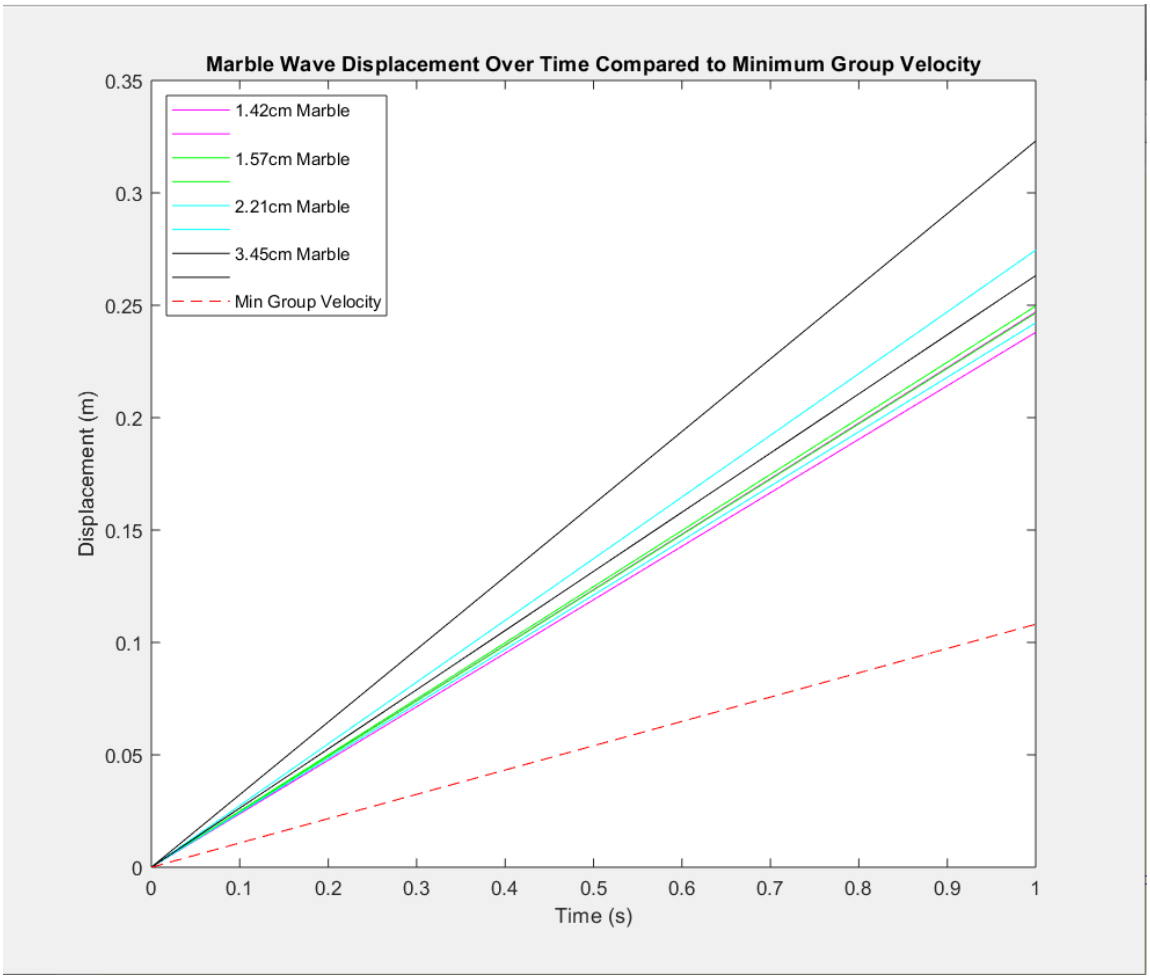

Figure 3: Wave displacement of experimental data plotted against the theoretical minimum result as a time series progression of wave displacement. Most important takeaway from this plot is the trajectory of experimental data group velocity existing above the minimum group velocity line (dotted in red).

2.5 Consistency Check

- Wave number (κ): $\frac{1}{m}$
- $\omega : Hz$
- Wavelength $lambda : m$
- Phase Speed $c_p : \frac{m}{s}$
- Group Speed $c_g : \frac{m}{s}$
- Surface Tension σ: Unitless... Traditionally this is found with units $\frac{N}{m}$ but in order to remove units, σ is divided by the density of water $\rho = 1000\frac{kg}{m^3}$ and $g = 9.81\frac{m}{s^2}$. The units cancel exactly in the resulting equation $\sigma = \frac{g}{\kappa^2}$.

2.6 Final Observation

After plotting our experimental data against theoretically derived values, we have outlined the logistics of dispersive wave propagation. Specifically looking at Figure 2 the relationship between individual wave (phase) velocity c_p and group velocity c_g has become clear. The curves of the two theoretical minimum function intersect at wave number $\kappa = 990.0m^{-1}$ and velocity $0.141\frac{m}{s}$ which correlates to a wavelength of 0.63cm. As mentioned before, these minimum value functions also help clarify the critical point of wave propagation speed relative to marble size. We found smaller waves propagated faster for all marble diameters except the largest, where the opposite was true.

3 SnodGrass Analysis

For the second half of our dispersive water waves investigation we have looked into a similar problem in a vary different setting. In the paper Sondgrass et. al wave propagation is measured across an entire ocean. Specifically four measurement devises– at Tutuila, Palmyra, Honolulu, and Yakutat islands- were conveniently spaced to span the distance between New Zealand and Alaska as shown in Figure 5.

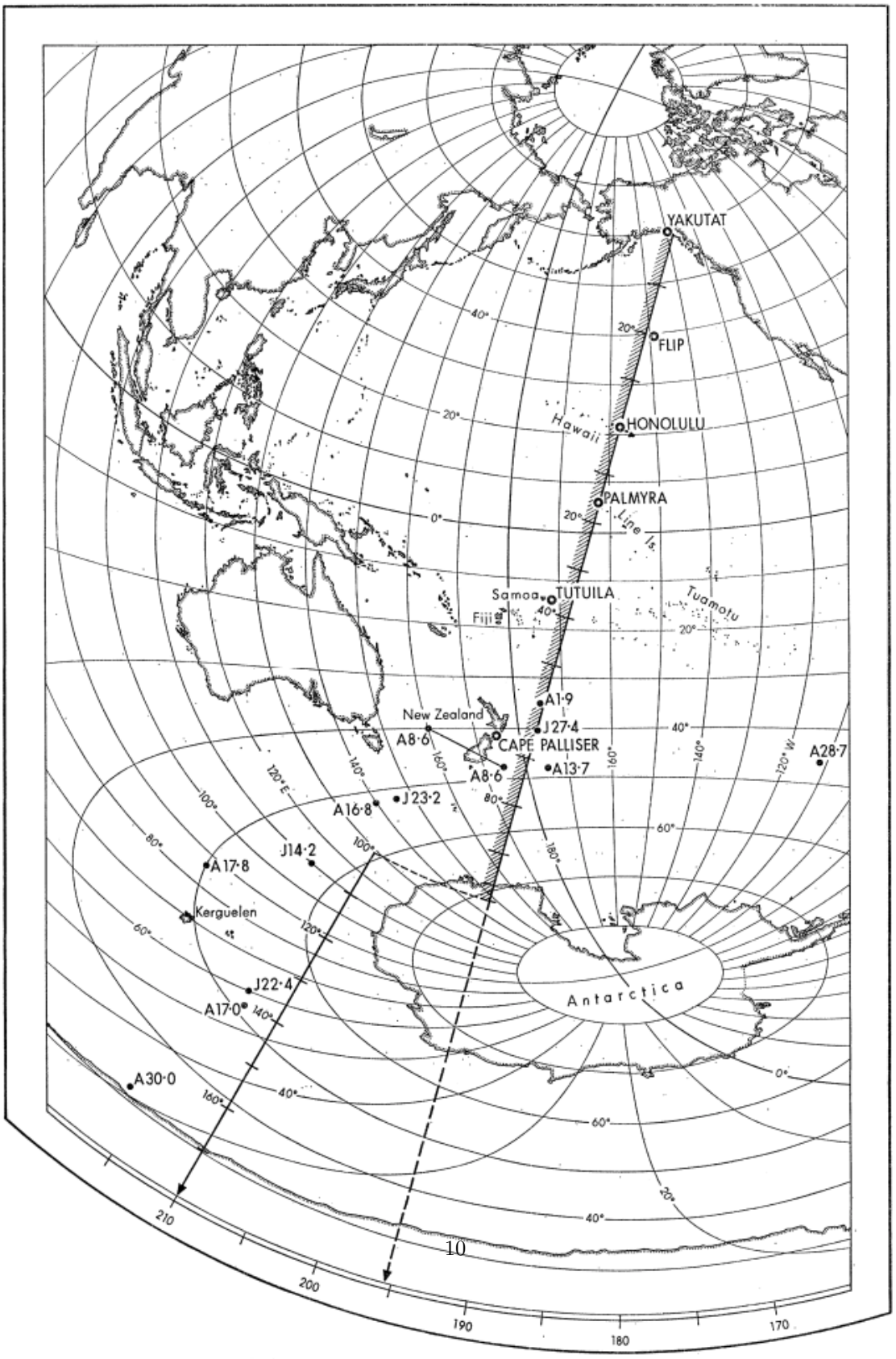

Figure 4: Taken from Figure 1 in Sondgrass et. al. This shows the physical layout of the measurement system designed to create a large-scale experiment of waves traveling across the entire ocean.

Water waves in the context of Earths many large bodies of water can be split into two different categories. "Seas" are waves that are generated by local winds. "swells" are waves generated elsewhere by a storm-like event, and this is the type of wave we will be assuming when investigating SnodGrass's experiment. Because swell waves are generated else where and are given plenty of distance to disperse, the waves tend to be well "synchronized". In the context of this experiment, this means that the frequency and intensity of the wave groups traveling past the four measurement locations will have stabilized and therefore unique to all the others.

3.1 SnodGrass Calculations

In this project we investigated two separate data sets from two swell wave occasions that traveled past the four measurement locations on the map. It is likely that both storm events occurred somewhere near Antarctica. To interpret the results from these two equations, we will follow three chosen waves that have clear characterizing frequencies through three or four of our measurement locations as shown:

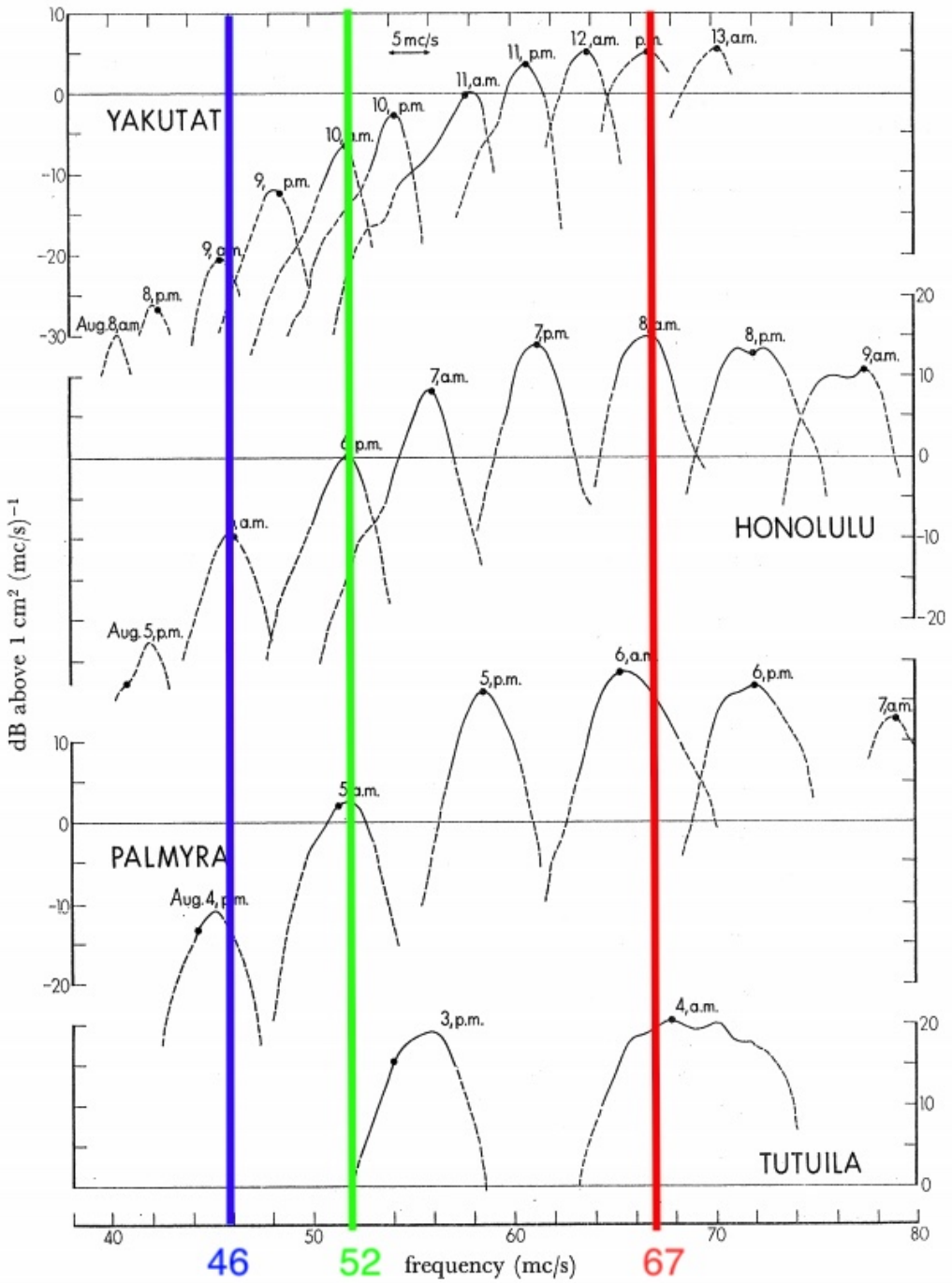

FIGURE 20. Successive spectra at the four stations for the event of 1·9 August. The dots correspond to the chosen ridge line for this particular event (see figure 16), and they are positioned relative to the bottom frequency scale. The spectra to either side are drawn on a compressed frequency scale to avoid overlap; the width of a 5 mc/s band is shown by the arrow.

Figure 5: Taken from Figure 20 in Sondgrass et. al. These are the results of the data collected at the four measurement locations. As seen in color we have chosen three waves to follow through the journey by finding frequencies that clearly identify a unique wave at three of the four locations. This was found by drawing a vertical line that passes through a peak intensity at all four locations.

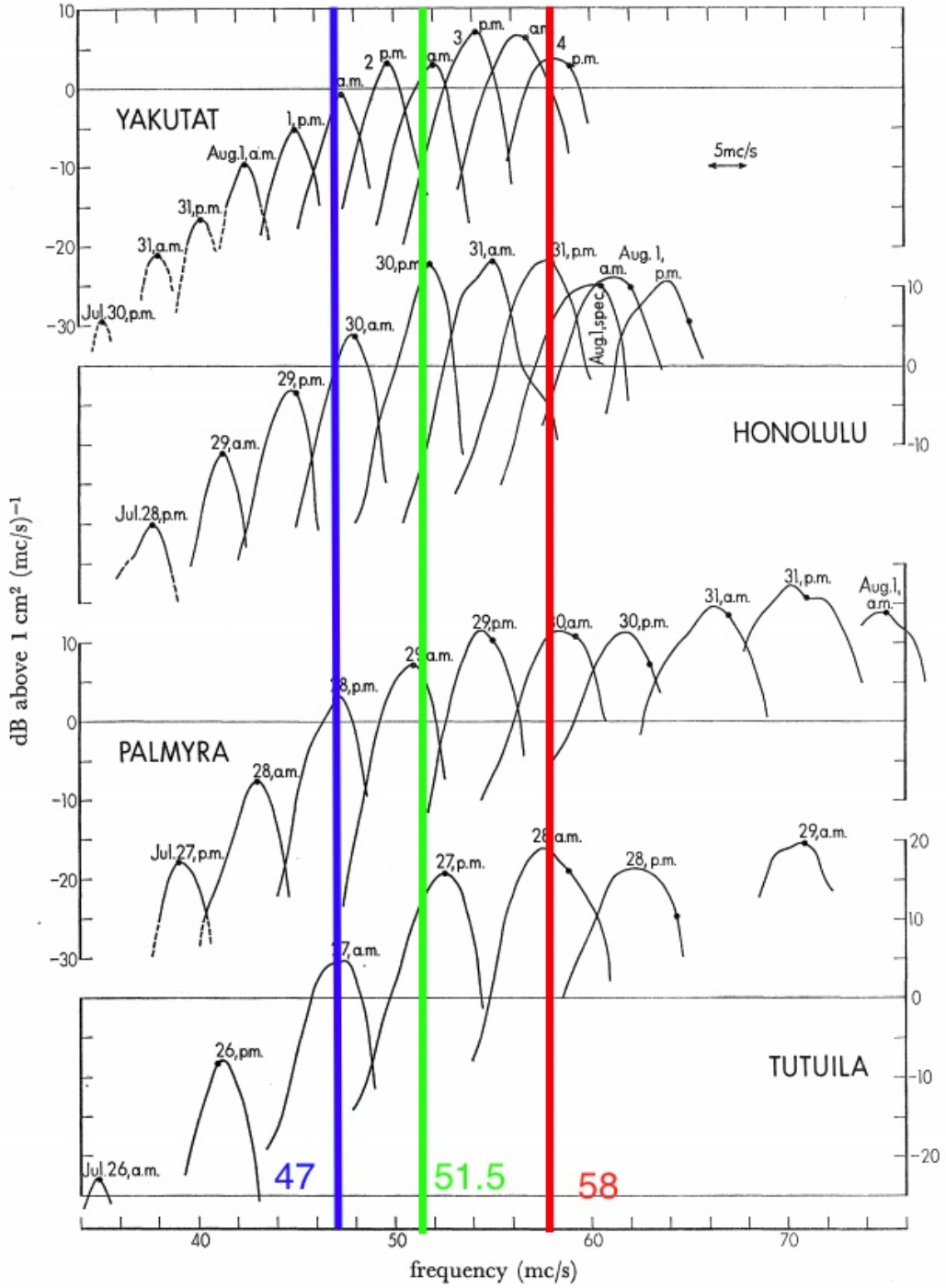

FIGURE 25. Successive spectra at the four stations for the event of 23·2 July. The dots correspond to the chosen position of the ridge line for this particular event (see figure 16), and they are positioned relative to the bottom frequency scale. The spectra to either side are drawn on a compressed frequency scale to avoid overlap; the width of a 5 mc/s band is shown by the arrow.

Figure 6: Taken from Figure 25 in Sondgrass et. al. Above again, are the results of the data collected at the four measurement locations during a new storm event. As seen in color we have chosen three waves to follow through the journey by finding frequencies that clearly identify a unique wave at all locations. This was found by drawing a vertical line that passes through a peak intensity at all four locations.

Having stationary locations to take measurements creates a new variation of calculations from our previous section that involved our own measurements. Because the ocean is so deep, we can approximate Eq. 2 with

$$\omega^2 = g\kappa$$

with $g >> \sigma$ and large h. When we additionally consider that $\kappa = \frac{2\pi}{\lambda}$, we can quickly rearrange this equation to find wavelength

$$\lambda = \frac{g}{2\pi f^2}$$

Through Eq. 4 and some algebra we also find that the theoretical group speed is

$$c_g = \frac{g}{4\pi f}$$

This will allow us to solve for a predicted "time of arrival" for our chosen waves at all of our desired measurement locations. Through a quick Google we have found that the distances between Tutuila, Palmyra, Honolulu, and Yakutat respectively is 1516miles, 1101 miles, and 2787 miles. By dividing these distances by the theoretical group velocity calculated from the formula above, we should get a fair prediction of the time it will take each wave to travel it's required distance.

For both storms occasions, our prediction of the time of wave arrival was perfectly within the 24hr margin of error allowed by the generality of the data given in Figures 5 & 6. For specific values see the correlated appended tables of results and error margins.

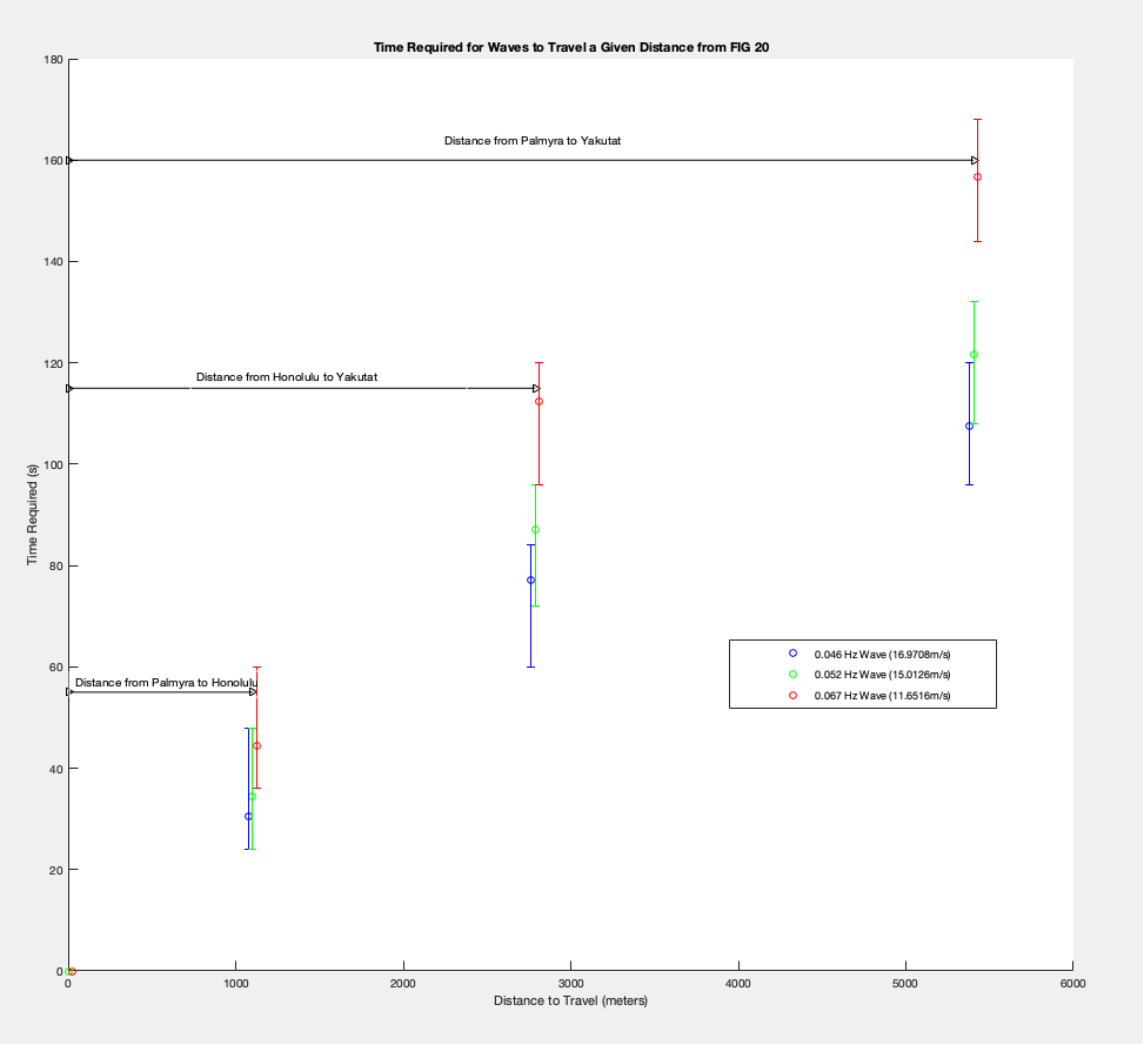

Figure 7: X-axis is distance required to travel and the y-axis is time it took to do so. With our three sets of wave propagation's, all of our theoretical values fell within the 24 error margin that result from the vague results of the experiment. Please note that the x-axis is strictly distance and it is not implied that the distance from one cluster of data to another is equivalent to the distance between two islands.

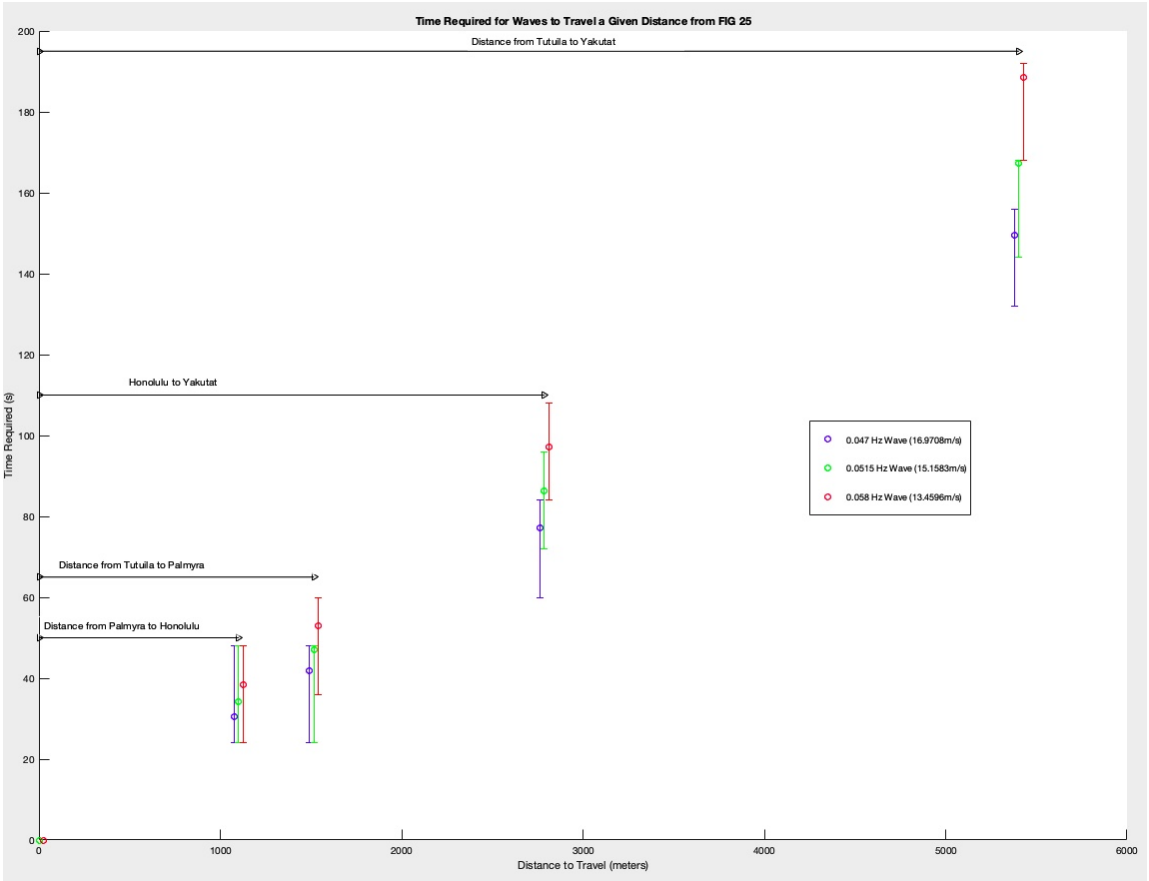

Figure 8: X-axis is distance required to travel and the y-axis is time it took to do so. With our three sets of wave propagation's, all of our theoretical values fell within the 24 error margin that result from the vague results of the experiment. Please note that the x-axis is strictly distance and it is not implied that the distance from one cluster of data to another is equivalent to the distance between two islands.

From these results we have outlined the power of tracking group velocity in the context of large distances and the deep ocean dispersion relation. We have accurately predicted the arrival interval of all of our chosen waves through through Eq. 4 and algebraic formulation.

4 Conclusion

The congregation of both our physical experiment alongside data from the SnodGrass et al. managed to simulated the generality and mechanics of a dispersion relation. In our personal experiment, we found the relationship between phase velocity and group velocity as well as got the opportunity to witness our capillary waves are created. Our significant results were a surface tension value of $0.01\frac{N}{m}$ as a result of non-ideal water. We also found final minimum group and phase velocity

function that are expressed thoroughly in Figure 2. In the analysis of the SnodGrass experiment we saw a contrasting solution of ocean water waves. We also experienced a similar but different version of measuring and tracking waves. Our results from this experiment all turned out to fall exactly in our windows of confidence based on our frequency tracking of long distance waves.

References

[1] Mei, C.C. CHAPTER FOUR. WAVES IN WATER. MIT - Department of Engineering, 2004

[2] 13.021 - Marine Hydrodynamics Lecture 19. MIT - Department of Engineering, 2004

[3] Snodgrass et al. Propagation of Ocean Swell Across the Pacific. Royal Society: London, UK. 1966

Appendix

4.0.1 SnodGrass Data

Frequency	Palmyra to Honolulu			Honolulu to Yakutat			Palmyra to Yakutat		
	Result	Err Min	Err Max	Result	Err Min	Err Max	Result	Err Min	Err Max
46	30.5	24	48	77.1	60	84	107.6	96	120
52	34.4	24	48	87.2	72	96	121.6	108	132
67	44.4	36	60	112.3	96	120	156.7	144	168

Table 1: From Fig 20 in Paper

Frequency	Tutuila to Palmyra			Palmyra to Honolulu			Honolulu to Yakutat			Palmyra to Yakutat		
	Result	Err Min	Err Max	Result	Err Min	Err Max	Result	Err Min	Err Max	Result	Err Min	Err Max
47	42.9	24	48	30.5	24	48	77.1	60	84	149.5	132	156
51.5	47.0	24	48	34.1	24	48	86.3	72	96	167.4	144	168
58	52.9	36	60	38.4	24	48	97.2	84	108	188.5	168	192

Table 2: From Fig 25 in paper